





Original Article


Special Issue on *Disaster Risk Reduction in Mountain Areas*


## Field observation of debris-flow activities in the initiation area of the Jiangjia Gully, Yunnan Province, China


**YANG Hong-juan**<sup>1</sup>  <https://orcid.org/0000-0003-0635-6764>; e-mail: yanghj@imde.ac.cn

**ZHANG Shao-jie**<sup>1\*</sup>  <https://orcid.org/0000-0001-5908-9554>;  e-mail: sj-zhang@imde.ac.cn

**HU Kai-heng**<sup>1</sup>  <https://orcid.org/0000-0001-8114-5743>; e-mail: khhu@imde.ac.cn

**WEI Fang-qiang**<sup>2</sup>  <https://orcid.org/0000-0001-8734-0881>; e-mail: fqwei@imde.ac.cn

**WANG Kai**<sup>1</sup>  <https://orcid.org/0000-0002-6593-7115>; e-mail: qianlimingyu@163.com

**LIU Shuang**<sup>1</sup>  <https://orcid.org/0000-0003-1990-5574>; e-mail: liushuang@imde.ac.cn

\*Corresponding author

<sup>1</sup> Key Laboratory of Mountain Hazards and Earth Surface Process, Institute of Mountain Hazards and Environment, Chinese Academy of Sciences, Chengdu 610041, China

<sup>2</sup> Chongqing Institute of Green and Intelligent Technology, Chinese Academy of Sciences, Chongqing 400714, China

**Citation:** Yang HJ, Zhang SJ, Hu KH, et al. (2022) Field observation of debris-flow activities in the initiation area of the Jiangjia Gully, Yunnan Province, China. *Journal of Mountain Science* 19(6). <https://doi.org/10.1007/s11629-021-7292-3>

© Science Press, Institute of Mountain Hazards and Environment, CAS and Springer-Verlag GmbH Germany, part of Springer Nature 2022

**Abstract:** The Jiangjia Gully, which is located in Dongchuan District, Yunnan Province, China, is a watershed prone to debris flows and has long-term recorded data of debris-flow occurrence. However, the initiation mechanism has mainly been studied by experiments in this watershed. To further reveal debris-flow formation mechanism in the Jiangjia Gully, debris-flow activities in the initiation zone were observed with hand-held video cameras in the summer of 2016 and 2017. In these two years, six debris-flow events were triggered in Menqian Gully, a major tributary of the Jiangjia Gully, while debris-flow activities in some sub-watersheds of Menqian Gully were recorded with video cameras in four events. The video recording shows that landslides constituted an important source for sediment supply in debris flow. Some landslides directly evolved into debris flows, while the others released sediment into rills and channels, where debris flows were generated for

sediment entrainment by water flow. Therefore, debris-flow occurrence in the Jiangjia Gully is influenced both by infiltration-dominated processes and by runoff-dominated processes. In addition, rainfall data from four gauges installed in Menqian Gully were analyzed using mean intensity ( $I$ ), duration ( $D$ ), peak 10-minute rainfall ( $R_{10min}$ ) and antecedent rainfall ( $AR$ ) up to 15 days prior to peak 10-minute rainfall. It reveals that debris-flow triggering events can be discriminated from non-triggering events either by an  $I$ - $D$  threshold or by an  $R_{10min}$ - $AR$  threshold. However, false alarms can be greatly reduced if these two kinds of thresholds are used together. Moreover, behaviors including intermittency of debris flow, variance in moisture content and volume among surges, and coalescence of multiple surges by temporary damming were observed, indicating the complexity of debris-flow initiation processes. These findings are expected to enhance our knowledge on debris-flow formation mechanism in regions with similar environmental settings.

**Received:** 24-Dec-2021

**Revised:** 02-Apr-2022

**Accepted:** 24-May-2022

**Keywords:** Debris flow; Field observation; Initiation mechanism; Rainfall threshold; Jiangjia gully

## 1 Introduction

Debris flows are gravity-driven mixtures of poorly sorted sediment, clasts and water with properties intermediate between floods and landslides (Iverson et al. 1997). They tend to occur in steep mountainous regions after intense or prolonged rainfall. The velocity of debris flow can be as high as 14 m/s, and the flow volume ranges from hundreds to millions of cubic meters (Rickenmann 1999). Therefore, debris flows may result in great economic loss and casualties for their destructive power. One example can be found in Zhouqu city in northwestern China on August 8, 2010, when a catastrophic debris flow destroyed more than 5500 houses and caused 1765 deaths (Tang et al. 2011). To mitigate debris-flow hazards, it is essential to understand the initiation mechanism of debris flow.

Debris-flow initiation requires an abundant source of unconsolidated material, steep terrain, and a source of moisture (Badoux et al. 2009). It has been recognized that debris flows are mainly triggered in two manners. On the one hand, landslides might mobilize to form debris flows (Johnson and Sitar 1990; Wang and Sassa 2007). Three processes have been revealed in the initiation of this type of debris flows: (1) widespread Coulomb failure within a soil mass, (2) partial or complete soil liquefaction by high pore fluid pressure, and (3) conversion of landslide translational energy to internal vibrational energy (Iverson et al. 1997). In terms of pore fluid pressure, controlled experiments show that it may increase dramatically (within 2–3 seconds) during slope failure because of soil contraction and agitation (Reid et al. 1997). On the other hand, debris flows can be generated by runoff, which is typical in alpine and recently burned areas (Kean et al. 2013). Two major classes of initiation mechanisms have been proposed for this type of debris flows. One is related with Coulomb failure of channel bed sediment (Takahashi 1978). The other is regarding sediment transport driven by hydrodynamic force (Gregoretti 2008). Diverse formulas have been given to calculate critical discharge triggering debris flows considering channel gradient and sediment grain size distribution (Tognacca et al. 2000; Gregoretti and Dalla Fontana

2008; Wang et al. 2017). In addition, debris flows may be initiated by outburst floods resulting from natural dams' failure (Takahashi 2007). If the flood entrains enough sediment from the dam itself or from the downstream channel, it will become a debris flow (Schuster 2000; Jiang et al. 2017).

Field observation of initiation processes of debris flow is the best way to study its formation mechanism. In recent years, in situ debris-flow monitoring has been conducted in many countries including Italy (Comiti et al. 2014; Simoni et al. 2020), the USA (Coe et al. 2008; Kean et al. 2011), Japan (Suwa et al. 1993; Imaizumi et al. 2019), China (Zhang 1993; Cui et al. 2018), Switzerland (Berger et al. 2011), Spain (Abancó et al. 2016), and France (Bel et al. 2017). Although most instruments are installed along downstream channels, some valuable data associated with debris-flow formation processes have been reported. Berti et al. (1999) reported a debris-flow event in the Dolomites, which initiated from the mobilization of in-channel debris and increased its volume by bed scouring and channel banks undercutting along the flow path. McCoy et al. (2012) found that bed sediment is entrained by debris flows from the sediment-surface downward in a progressive fashion and time-averaged entrainment rate is affected by sediment wetness. Kean et al. (2013) observed that debris flows at Chalk Cliffs can be generated by periodical release of accumulated sediment transported by water flow in lower gradient channels. Data from Ohya landslide show that partly saturated flow, which has an unsaturated layer in its upper part, is the predominant flow type in the steep initiation zone (Imaizumi et al. 2019).

As debris flows occur frequently in the Jiangjia Gully, it is an ideal location for in situ monitoring of debris flows. Field observation has been conducted in this basin by Chinese Academy of Sciences since 1965 (Zhang 1993), which provides long-term recorded data for debris-flow study in China (e.g., Zhuang et al. 2015; Wang et al. 2018). However, field observation data regarding the initiation zone are scarce except for precipitation, and the initiation mechanism has mainly been studied by experiments (Chen et al. 2006; Chen et al. 2010), in which the transformation of debris flows from landslides is emphasized. The specific object of this study is to reveal debris-flow initiation mechanism in the Jiangjia Gully by observing debris-flow activities in the initiation zone with hand-held video cameras and by analyzing

rainfall conditions responsible for observed debris-flow events.

## 2 Study Area

The Jiangjia Gully is a 48.6-km<sup>2</sup> watershed situated in Yunnan Province, southwestern China, with a geographical location of 103°05'46"–103°13'01"E and 26°13'16"–26°17'13"N. It has an elevation range of 1040–3260 m, with the landform generally inclining from east to west (Fig. 1). Terrain is steep in this basin, with slopes greater than 25° accounting for 68%. Gentler slopes are present close to the divides. Menqian Gully and Duozhao Gully are the two largest tributaries, accounting for 64.7% in drainage area. They also constitute the major zones for debris-flow initiation in the Jiangjia Gully. The U-shaped main stream channel downstream of the confluence of the two tributaries has a width of more than 100 m, and the gradient decreases from 5.1° in the transport zone to 3.7° in the deposition zone (Cui et al. 2005). In contrast, channels of the tributaries are commonly narrow and V-shaped, with inclinations greater than 8.5°.

The geological conditions of the Jiangjia Gully are strongly affected by the Xiaojiang fault, which runs across this area predominantly in a north-south

direction (Fig. 1). As the boundary between the active Sichuan-Yunnan block and the stable Yangtze block, the Xiaojiang fault is one of the most active and earthquake-prone faults in China (Liu et al. 2020). More than 10 earthquakes of  $M \geq 6$  have occurred along this fault since 1500 (Shi and Wang 2017). Due to intense tectonic activities, fractures are well developed in the Jiangjia Gully. Therefore, exposed bedrocks, mainly constituted by slates formed in lower Proterozoic, are fragmented, usually disintegrating into gravels of 20–100 mm (Fig. 2a). Gully incision is intense because of steep terrain and fractured bedrocks, and has caused extensive landsliding (Fig. 2b).

This area is characterized by subtropical monsoon climate. Mean annual rainfall varies from 400 to 1000 mm, and generally increases with elevation. About 85% of rainfall concentrates in the rainy season (May–October). Croplands are mainly distributed on gentler hillslopes (<25°) near the divides and on the alluvial fan. Some steeper hillslopes are covered by sparse shrubs or grass, while the others are barren for frequent failures. The soil mantle, with thicknesses of 0.5–20 m, is generally poorly-graded, and the particles range from clay to boulders. Rill and gully erosion are also active on steeper hillslopes (Fig. 2c).

To monitor debris-flow activities in the Jiangjia

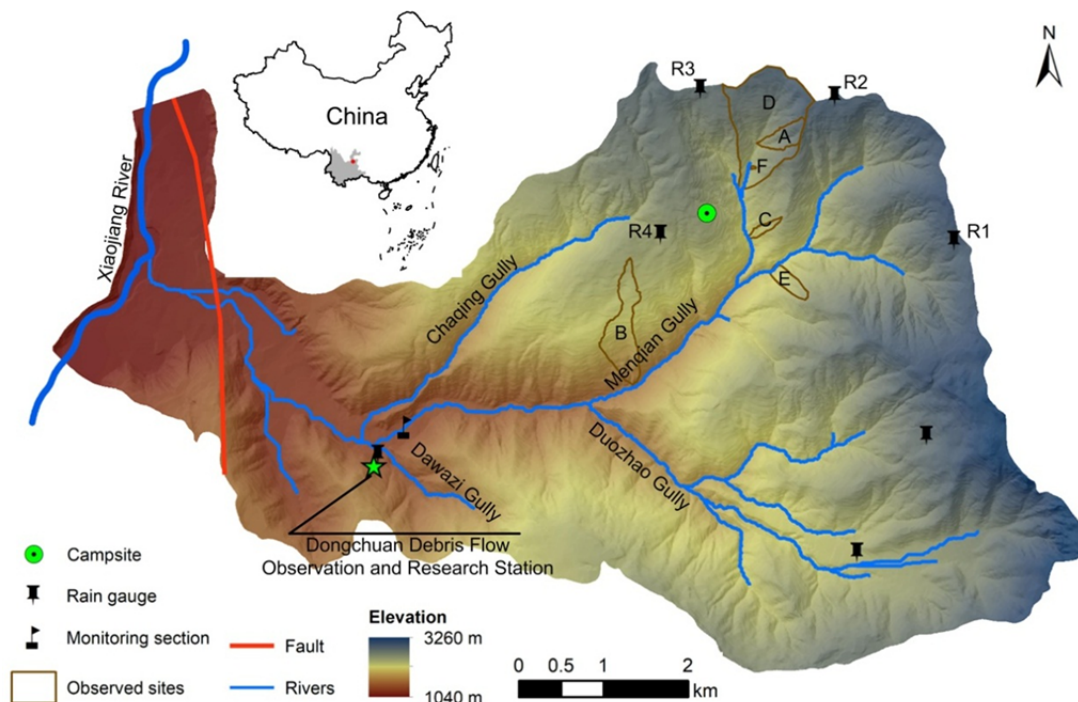


**Fig. 1** Location and terrain of the Jiangjia Gully.

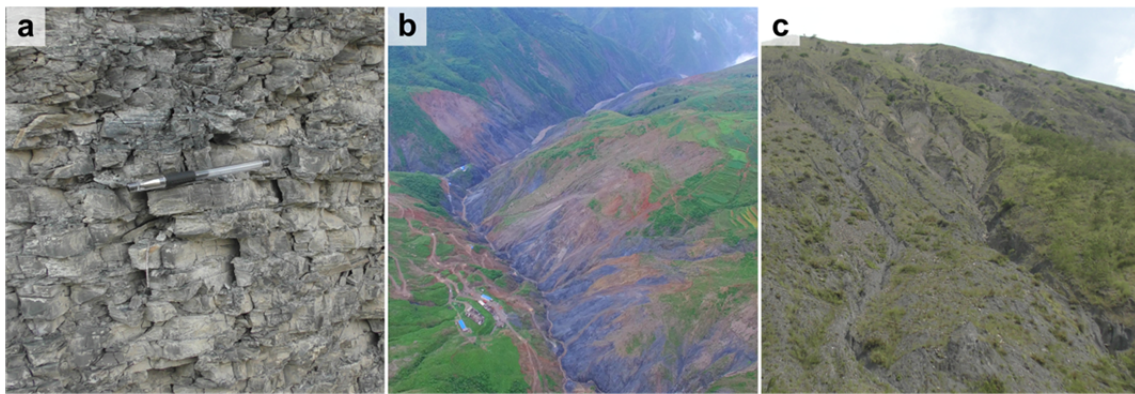


**Fig. 2** Photographs showing the fragile exposed bedrock (a), widespread landslides (b), and dense rills and gullies (c) in the Jiangjia watershed.

Gully, seven rain gauges were installed in the watershed by Dongchuan Debris Flow Observation and Research Station (DDFORS), while a monitoring section was built 2.2 km downstream of the confluence of Menqian Gully and Duo Zhao Gully (Fig. 1) to measure the depth and velocity of debris flow. Information on more than 500 debris-flow events has been recorded (Guo et al. 2020), which shows that a high-intensity rainfall event lasting for 10–20 minutes can trigger a debris flow (Zhuang et al. 2015).

### 3 Data and Methodology

Methods including video recording, field survey and rainfall analysis were employed in this study. Due to the construction of check dams in Duo Zhao Gully, debris flows observed in the main channel of the Jiangjia Gully are primarily discharged from Menqian Gully currently. Therefore, our study was focused on this tributary. A campsite was set up in the initiation zone of Menqian Gully in 2016 (Fig. 1). Some observers lived at the campsite during July 13–August 21 in 2016 and July 13–August 26 in 2017 to record debris flows triggered on hillslopes and in channels in the vicinity of the campsite using video cameras. A single observation usually lasted for tens of minutes. The observation was discontinuous for the impact of fog. Once debris flows were recorded near the campsite, observers staying at DDFORS would check if there were fresh debris-flow deposits in the main channel of the Jiangjia Gully after the rain. That is to say, only events with debris flows arriving at or moving farther than the outlet of Menqian Gully were labeled as debris-flow events in Menqian Gully. In addition, field survey was aperiodically carried out to

investigate geomorphic features, such as distribution of unconsolidated material and groundwater outcrop, at the sites where debris flows were recorded.

Digital elevation model (DEM) data, digital orthophoto, and rainfall data provided by DDFORS were also used in this study. The high-resolution (0.17 m) DEM data and digital orthophoto, obtained in December 2017 with aerial photogrammetry using an unmanned aerial vehicle, were employed to derive topographic map, slope distribution, channel length and gradient of interested sites. Rainfall data monitored at 1-minute intervals by the four tipping bucket rain gauges installed in Menqian Gully, which were denoted by R1 through R4 in Fig. 1, were used for rainfall analysis. The measurement accuracy is 0.1 mm. Gauge R2 was out of order in 2017, thus only data from the remaining gauges were available this year.

The power-law function between mean intensity ( $I$ ) and duration ( $D$ ), i.e.,  $I = \alpha \cdot D^\beta$ , has been widely used in defining rainfall threshold for debris flows and shallow landslides (e.g., Guzzetti et al. 2008; Bel et al. 2017), where  $\alpha$  is the scaling coefficient and  $\beta$  is the exponent of the power function. Moreover, the linear function between peak 10-minute rainfall ( $R_{10min}$ ) and antecedent rainfall prior to the occurrence of peak 10-minute rainfall ( $AR$ ), i.e.,  $R_{10min} = a + b \times AR$ , where  $a$  is the intercept and  $b$  is the slope of the linear function, has been employed to predict debris-flow occurrence in the Jiangjia Gully (Zhang 1993). Therefore, the four parameters including  $I$ ,  $D$ ,  $R_{10min}$ , and  $AR$  were calculated for each rainfall event in the observation period. Among them, antecedent rainfall was computed with the following equation:



$$AR = \sum_{i=1}^n k^i R_i + R_0 \quad (1)$$

where  $R_i$  is rainfall accumulated in the  $i$ -th 24 hours prior to the rainfall event;  $R_0$  is rainfall accumulated from the beginning of the event to the occurrence of peak 10-minute rainfall;  $n$  is the number of days considered; and  $k$  is the decay factor. Suggested values for  $n$  and  $k$  are 15 and 0.78 respectively (Zhuang et al. 2015).

The selection of inter-event time (IET), which corresponds to the minimum duration of no rain gap between two contiguous rainfall events, is crucial when defining a rainfall event (Bezák et al. 2016). There are no standard criteria for selecting IET (Jiang et al. 2021). In this research, we analyzed the histogram of the duration of no rain gaps following Bel et al. (2017) to determine this value. Using rainfall data recorded by the four gauges in the rainy season of 2016 and 2017, the number of no rain gaps with different durations was calculated, as illustrated in Fig. 3. It decreases sharply when the duration is shorter than 5 h while diminishing more gently when the duration is longer than 5 h, indicating that rainfall events with shorter no rain gaps were most likely episodes of events with longer no rain gaps. Therefore, 5 h was chosen for IET in this study.

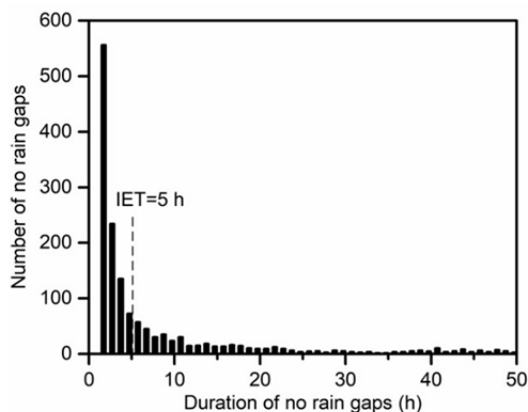


**Fig. 3** Histogram of the duration of no rain gaps calculated with rainfall data collected by gauges R1-R4 in the rainy season of 2016 and 2017.

Rainfall events in the observation period were divided into two groups: debris-flow triggering events and non-triggering events. To define the  $I$ - $D$  threshold ( $I = \alpha \cdot D^\beta$ ) for debris flow, the gauge with highest  $I$  and  $D$  values was selected as the representative gauge for each rainfall event, because debris flows most likely initiated in the area (s)

neighboring this gauge. Then the exponent ( $\beta$ ) in the threshold was determined by logistic regression (Giannecchini et al. 2016; Bel et al. 2017). For each debris-flow triggering event, the scaling coefficient ( $\alpha$ ) was calculated using corresponding  $I$  and  $D$  values. The smallest one was finally selected for rainfall threshold definition. The  $R_{10min}$ - $AR$  threshold ( $R_{10min} = a + b \times AR$ ) was defined using the same procedure.

## 4 Results

### 4.1 Rainfall conditions responsible for debris flows in Menqian Gully

Six debris-flow events were triggered in the main channel of Menqian Gully in 2016 and 2017. Out of them, four events were triggered during observers' stay at the campsite, with two events occurring on August 14, 2017 and the other two occurring on August 10, 2016 and August 25, 2017 separately. These four events all had relatively short runoff distances. Specifically, debris flows arrived 1.4 km downstream of the outlet of Menqian Gully in the second event on August 14, 2017 while debris flows arrived at the outlet of Menqian Gully in the remaining three events. Therefore, they were not recorded at the monitoring section of DDFORS. Great variance usually existed in accumulated event rainfall measured by different gauges. Event rainfall was 6.1-19.8 and 12.7-90.1 mm for the August 10, 2016 and August 25, 2017 debris-flow events respectively (Fig. 4a, 4e). For the two events on August 14, 2017, cumulative rainfall was 6.6-32.2 and 12.8-29.9 mm separately (Fig. 4d). In these rainfall events, debris flows were observed in three sub-watersheds (denoted by A, C, and D in Fig. 1) and on two slopes (denoted by E and F in Fig. 1) at the campsite. Fig. 4a, 4d, 4e illustrated the moment that debris flows were detected, which was generally in the time period when cumulative rainfall increased rapidly except for Fig. 4e.

Two debris-flow events occurred in Menqian Gully before observers' stay at the campsite in 2017, and thus they were not recorded by hand-held video cameras. However, they were observed at the monitoring section on July 3, 2017 and July 7, 2017 separately, with 46 and 30 debris surges recorded correspondingly. Runout distances of these two

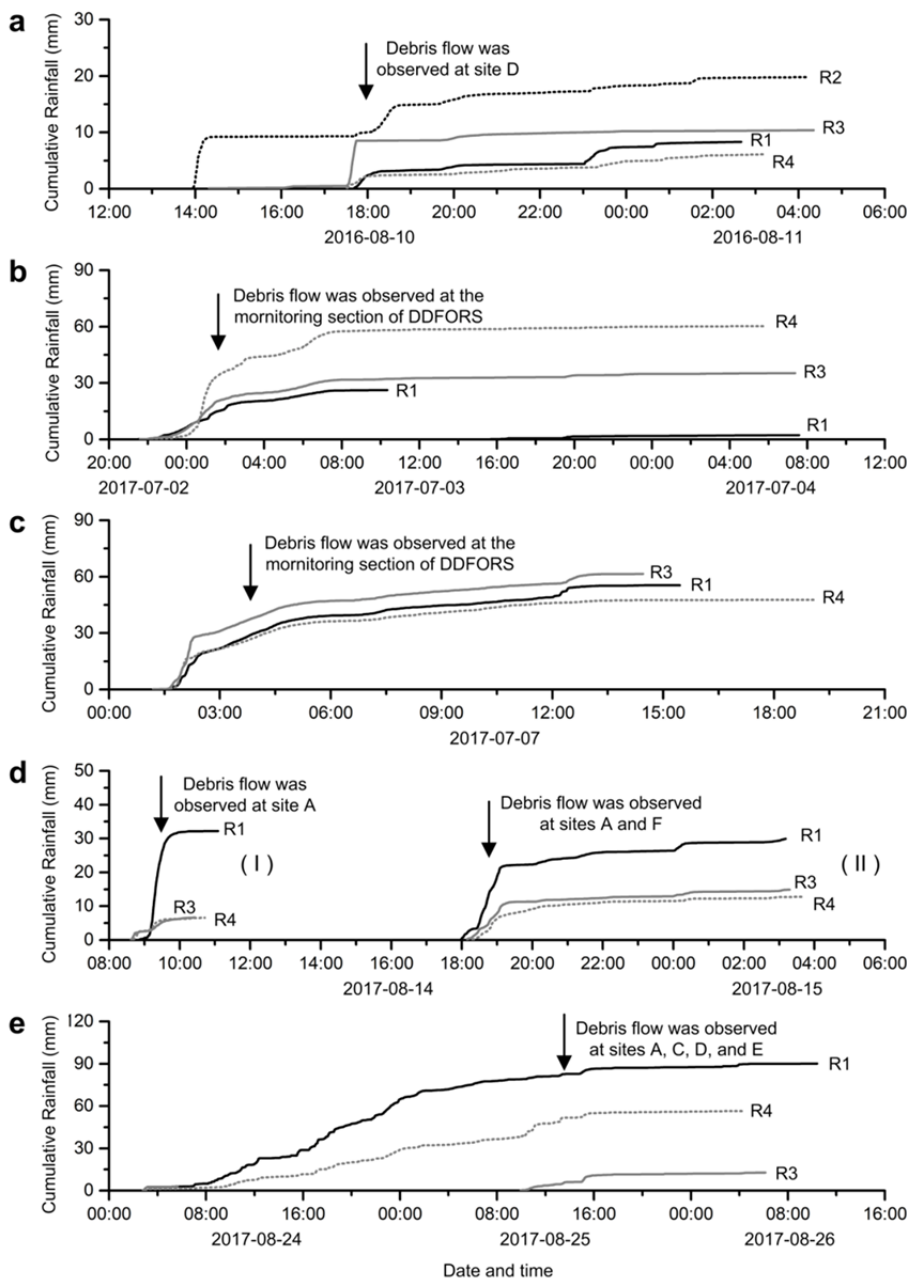


**Fig. 4** Cumulative rainfall measured by available gauges for the 6 debris-flow events triggered in Menqian Gully in 2016 and 2017. Two debris-flow events occurred on August 14, 2017, with the corresponding rainfall denoted by I and II separately (d). Gauge R2 was out of order in 2017 and no rainfall data were collected.

events were evidently longer than the above-mentioned four events. The associated rainfall data were shown in Fig. 4b, 4c. Accumulated event rainfall was 26.2–60.2 mm on July 3, 2017, and also exhibited great difference among gauges. The difference was much smaller on July 7, 2017, and event rainfall was 47.7–61.5 mm.

Parameters including  $I$ ,  $D$ ,  $R_{10min}$ , and  $AR$  were

computed for the six rainfall events using data from each gauge, as listed in Table 1. They were also calculated for the remaining 44 rainfall events occurring in the observation period that did not trigger debris flows in the main channel of Menqian Gully. Using the method described in section 3, the  $I$ - $D$  threshold and the  $R_{10min}$ - $AR$  threshold for debris flow were determined respectively, with  $I = 12.27D^{-0.82}$  and  $R_{10min} = 13.60 - 0.26AR$ , as illustrated in Fig. 5. Generally, both thresholds can effectively distinguish triggering events from non-triggering ones, with 3 and 4 false alarms separately. Interestingly, only one non-triggering event exceeds both thresholds, suggesting that these two thresholds can be used together to reduce false alarms. In addition, rainfall data recorded by all available gauges exceed the two thresholds in the July 3, 2017 and July 7, 2017 flow events, while data recorded by 1 or 2 gauges surpass the two thresholds in the other events, indicating that debris flows were most likely widely triggered in the sub-watersheds of Menqian Gully in the former two

events, and the total volume of debris flow was so large that the debris could propagate farther than the monitoring section.

#### 4.2 Debris-flow activities observed in the initiation area

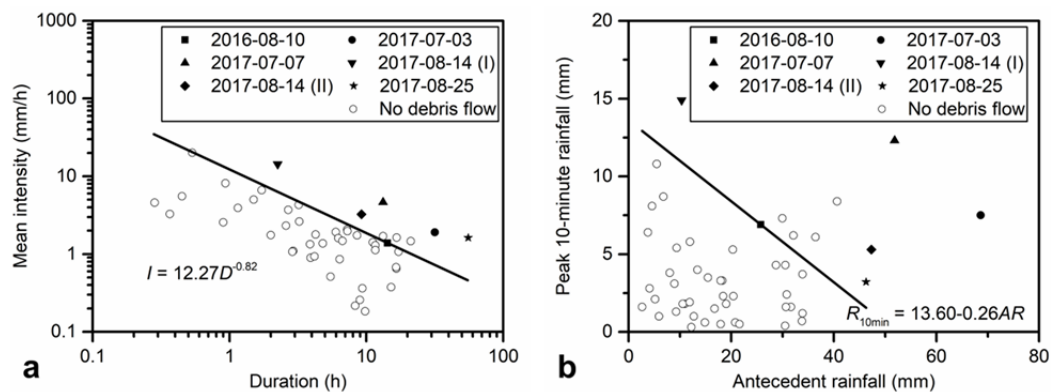
In the observation period, debris-flow activities

**Table 1** Rainfall conditions for the recorded debris-flow events in Menqian Gully

Date (yyyy-mm-dd)	Rain gauge	Event rainfall (mm)	Duration (h)	Mean intensity (mm/h)	Peak 10-minute rainfall (mm)	Antecedent rainfall (mm)
2016-08-10	R1	8.3	9.00	0.92	1.7	28.0
	R2	19.8	14.27	1.39	6.9	25.8
	R3	10.4	14.05	0.74	7.4	13.7
	R4	6.1	9.72	0.63	1.0	12.3
2017-07-03	R1	26.2	12.87	2.04	2.2	82.6
	R3	35.2	33.80	1.04	2.6	79.5
	R4	60.2	31.72	1.90	7.5	68.7
2017-07-07	R1	55.5	13.90	3.99	6.1	42.9
	R3	61.5	13.28	4.63	12.3	51.9
	R4	47.7	17.62	2.71	10.5	45.9
2017-08-14 (I)	R1	32.2	2.25	14.31	14.9	10.3
	R3	6.7	1.83	3.66	2.1	3.9
	R4	6.6	2.07	3.19	2.3	6.1
2017-08-14 (II)	R1	29.9	9.23	3.24	5.3	47.3
	R3	14.9	9.17	1.62	2.7	18.1
	R4	12.8	9.43	1.36	2.8	15.0
2017-08-25	R1	90.1	55.53	1.62	2.9	41.8
	R3	12.7	20.22	0.63	2.1	15.6
	R4	56.5	49.37	1.14	3.2	46.3

**Table 2** Occurrence sites and date of debris flows observed with hand-held video cameras

Site	Date	Position of observers
Sub-watershed A	2017-07-15, 2017-07-16, 2017-08-14, 2017-08-25	At the campsite
Sub-watershed B	2017-07-23	At the outlet of sub-watershed B
Sub-watershed C	2017-08-25	At the campsite
Sub-watershed D	2016-08-10, 2017-08-25	At the campsite
Slope E	2017-08-25	At the campsite
Slope F	2017-08-14	At the campsite

**Fig. 5** The  $I$ - $D$  threshold (a) and  $R_{10min}$ - $AR$  threshold (b) for debris-flow triggering in Menqian Gully using data recorded in 2016 and 2017.

at six sites, denoted by A through F in Fig. 1, were recorded by hand-held video cameras in the initiation zone. Some were triggered by the rainfall events illustrated in Fig. 4, while the others were triggered by rainfall events without accompanying debris flows in the main channel of Menqian Gully, as listed in Table 2. Video recordings related with sub-watersheds A, B, and C were presented because they were less affected by fog.

#### 4.2.1 Sub-watershed A

Sub-watershed A is situated in the northeastern part of the Jiangjia Gully, denoted by A in Fig. 1. It has a drainage area of 0.10 km<sup>2</sup> and a relative relief of 421 m (2256-2677 m a.s.l.), with an unpaved road crossing the middle part at an elevation of ~2500 m. Terrain is steep in this area, with slopes below the elevation of 2620 m generally greater than 30°. The

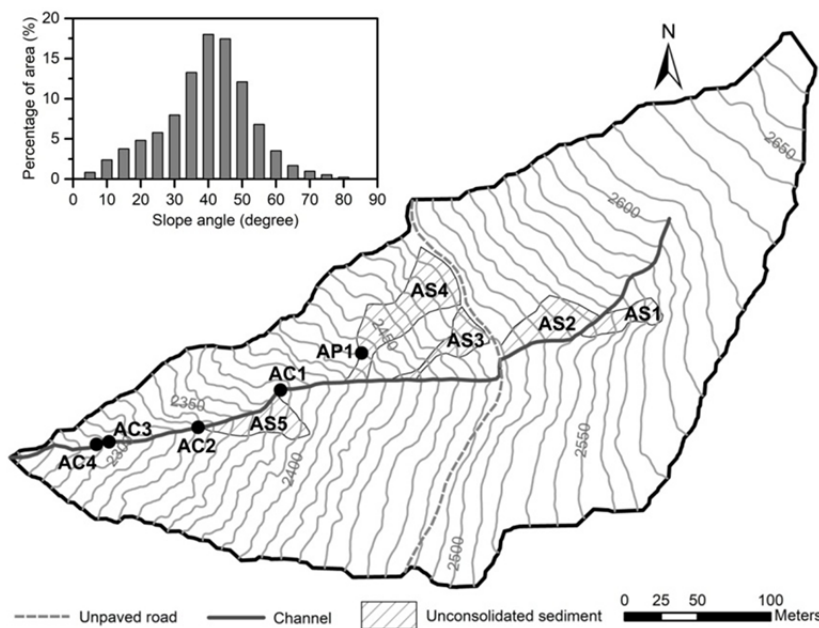


**Fig. 6** Terrain of sub-watershed A.

534-m-long channel has a mean gradient of  $33.2^\circ$ . The reach upstream of the road is filled with sediment while seasonal runoff is present in the downstream reach. Shallow landslides are widely distributed along the channel and the road. No debris flows were triggered in the channel in the August 10, 2016 rainfall event, whereas fresh debris-flow deposits caused by rill erosion were observed on some slopes. The intense rainfall in early July in 2017 triggered new landslides along the road. The mobilized sediment was deposited on hillslopes downstream of the road and provided additional loose material for debris-flow formation. Fig. 6 illustrates the five main sites storing unconsolidated sediment along the channel observed on July 13, 2017. Debris flows occurred in this sub-watershed in the August 14, 2017 and August 25, 2017 rainfall events. Moreover, debris flows were observed in this area on July 15-16, 2017, which were presented below. The corresponding rainfall data measured by the nearest gauge available (R3) were shown in Fig. 7. The rain mainly occurred during 0:00-2:00 and 7:00-9:00 on July 15, with a peak 10-minute rainfall of 4.3 mm. This flow event was characterized by long duration (over 29 hours) and intermittent flows, with sediment provided by areas AS3-AS5.

The observation on July 15 lasted from 11:34 to 12:13. In the beginning, the granular front of the flowing mass was detected at section AC4, ~64 m upstream of the outlet. It traveled forward

intermittently, and the mean velocity was small ( $\sim 0.05$  m/s). When it moved downstream, gravels located on the steep surface rolled or slid downslope and fell on the channel bed. Behind the front part, debris flows only propagated in the central part of the channel, while debris on the two sides stayed still, suggesting that lateral levees had been formed (Fig. 8a). A levee collapse induced by debris-flow erosion was observed at 11:45, indicating that levees could provide sediment to passing debris surges. In the observation period, five debris surges were detected between sections AC1 and AC2, all of which were

composed of a granular snout and a muddy tail and traveled much faster than the above-mentioned front. For instance, the surge observed at 11:36 moved at a velocity of  $\sim 0.6$  m/s. Debris-flow activities in the reach upstream of section AC1 was out of sight, impeding a direct observation of debris-flow formation process. In terms of hillslopes, mass movement was also active. At 11:34, scars caused by slope failures were present in regions AS3 and AS4 (Fig. 8b). In the 39-minute observation period, small failures extending for tens of centimeters occurred frequently in regions AS4 and AS5, with most mobilized sediment resting on downstream slopes after traveling a short distance (less than 5 m), whereas a small part of sediment directly entering the channel.

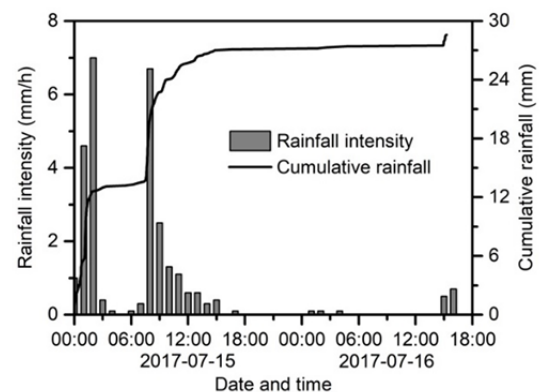


**Fig. 7** Rainfall intensity at 1-hour intervals and cumulative rainfall recorded by R3 on July 15-16, 2017.



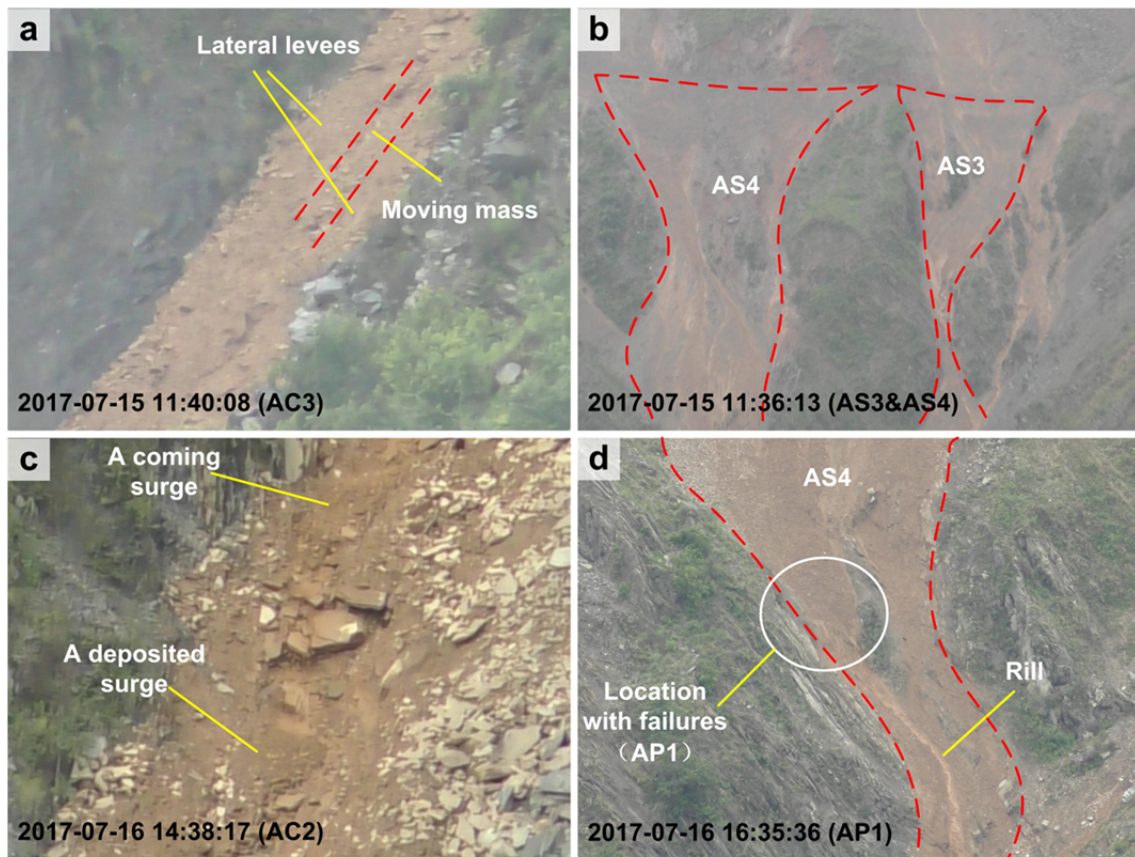


**Fig. 8** Video images showing lateral levees formed by debris flow (a), and scars of slope failures in areas AS3 and AS4 (b) on July 15, 2017, coalescence of multiple surges (c) and location with failures in area AS4 (d) on July 16, 2017 in sub-watershed A. Location of the framed area is listed in the bracket.

The observation on July 16 comprised two time periods: 14:28-14:47 and 16:33-17:18. In the first period, the process of combination of smaller debris surges into a larger one was recorded. At 14:38, a debris surge stopped downstream of a step near section AC2 (Fig. 8c). The next two surges also came to rest when arriving at this position. With the arrival of the fourth surge, the deposited mass was restarted, becoming a larger debris surge. In addition, a small collapse was triggered by debris-flow erosion at the toe of slope AS5 at 14:33. In the second period, small failures frequently occurred at the toe of a patch of sediment in area AS4 (Fig. 8d). Some mobilized sediment entered the downstream rill, and was released as small surges of debris flow afterwards.

#### 4.2.2 Sub-watershed B

The 0.36-km<sup>2</sup> sub-watershed B is located near the outlet of Menqian Gully, with a relative relief of 671 m (1614-2285 m a.s.l.) and an accumulation fan of 31 827 m<sup>2</sup>, denoted by B in Fig. 1. The 472-m-long main channel can be divided into two reaches

according to gradient, with the reach upstream of BC1 of 27.8° and the remaining reach of 20.8°. The channel is formed on a large landslide, the scarp of which is located at an elevation of ~2070 m. Some secondary landslides have been developed for gully erosion, with the scarps illustrated in Fig. 9. Therefore, hillslopes along the main channel are primarily comprised by landslide deposits and are prone to gully erosion in rainy seasons (Appendix 1). Debris flows are so active in this sub-watershed that they can occur even on non-rainy days.

Debris-flow activities in sub-watershed B were recorded during 9:50-11:00 on July 23, 2017, with no rainfall measured by the nearest gauge (R4) in the past 24 hours. Five main phenomena were observed. Firstly, intermittent debris flows resulted from intermittent bank collapses. For instance, during the period 10:04:23-10:05:07, inflow at section BC2 remained as water flow (Fig. 10a). Bank collapses occurred between sections BC2 and BC3 at 10:04:24, 10:04:31, and 10:04:41, respectively. Correspondingly, snouts of debris flows were observed at section BC3 at

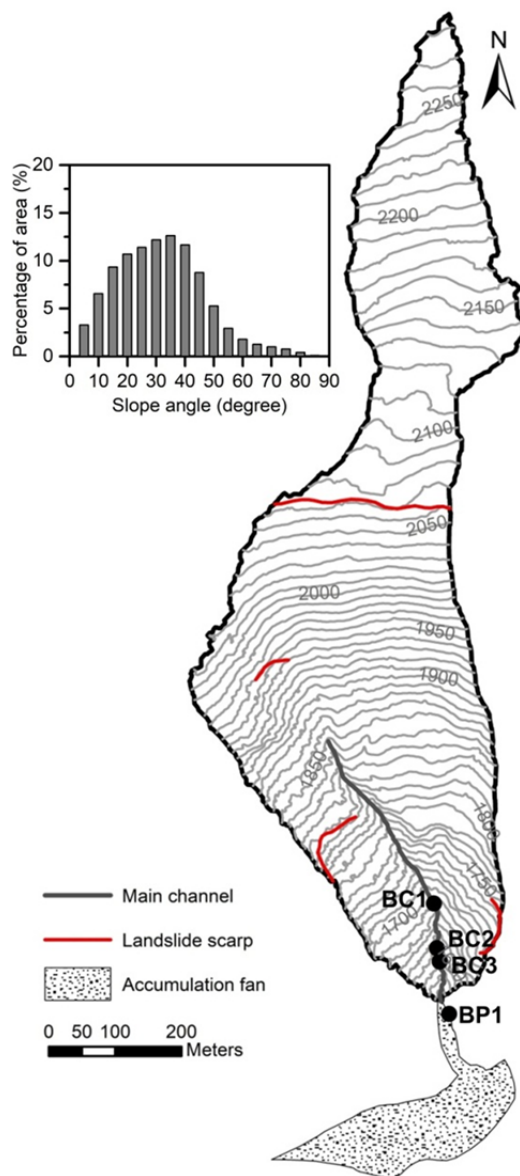


**Fig. 9** Terrain of sub-watershed B.

10:04:30, 10:04:39, and 10:04:55. In addition, the process that debris flows were generated by small outburst floods was observed. When the channel was blocked by a collapse, incoming water initially accumulated upstream of the block body, and then overtopped it and eroded the downstream face, thus forming a surge of debris flow. Moreover, significant variance was present in the volume of different debris surges. For instance, the three aforementioned surges observed at section BC3 lasted for less than 10 s. In contrast, another surge observed at 10:34 lasted for more than 40 s and had greater flow depth (Fig. 10b). Furthermore, both partly saturated flows and fully saturated flows were observed. Debris flows moved

relatively slowly when they entered the accumulation zone, making it easy to identify whether the flow was fully saturated. The debris surge observed at 10:14 at BP1 was fully saturated (Fig. 10c) while fluid was invisible at the surface of the surge observed at 10:22 (Fig. 10d). Besides, transport behaviors of the solid fraction in the flow were associated with particle size. Gravels with sizes far smaller than flow depth “floated” in the flow, while boulders having sizes comparable to flow depth moved by rolling (not illustrated).

#### 4.2.3 Sub-watershed C

Sub-watershed C has a drainage area of 0.033 km<sup>2</sup> and a relative relief of 369 m (1919–2288 m a.s.l.), denoted by C in Fig. 1. The channel is 131 m long, with a mean slope of 35.7°. Groundwater outcrops in the concave area near the source of the channel and constitutes tiny baseflow in rainy season. A landslide scarp is present at the elevation of ~2170 m. Masses of unconsolidated material are stored on the hillslope downstream of the scarp. Besides, landslides are active along the unpaved road, generating additional loose sediment on the hillslope. Fig. 11 illustrates the four main areas with sediment storage (CS1–CS4). Debris-flow activities in this sub-watershed were observed during 13:39–16:03 on August 25, 2017, with the associated rainfall data illustrated in Fig. 12. The main process of debris-flow formation was that failures or rill erosion occurred on some slopes, initially generating intermittent granular flow or debris flow in the rill and finally forming debris surges in the channel.

A surge of debris flow was observed in the channel at 13:39 (Fig. 13a), which was the largest one in volume recorded in the observation period, with the flowing mass looking viscous. This debris surge was traced back to slope CS4, where debris flow was propagating to the channel through a rill. Debris-flow activity on this slope weakened after 13:47. However, with the arrival of a new rainfall burst at 14:57, it became active again, which was primarily caused by rill erosion. Only one rill was observed on the slope at 13:41 (Fig. 13b) while more rills were present at 15:37 (Fig. 13c). In addition, small failures extending for tens of centimeters also contributed to debris-flow occurrence on this slope. Two failures were recorded during the observation period, sediment mobilized by which was quickly moved by water flow in the rill.

Mass movement was also found on other slopes connected with the channel. At 13:40, a small collapse



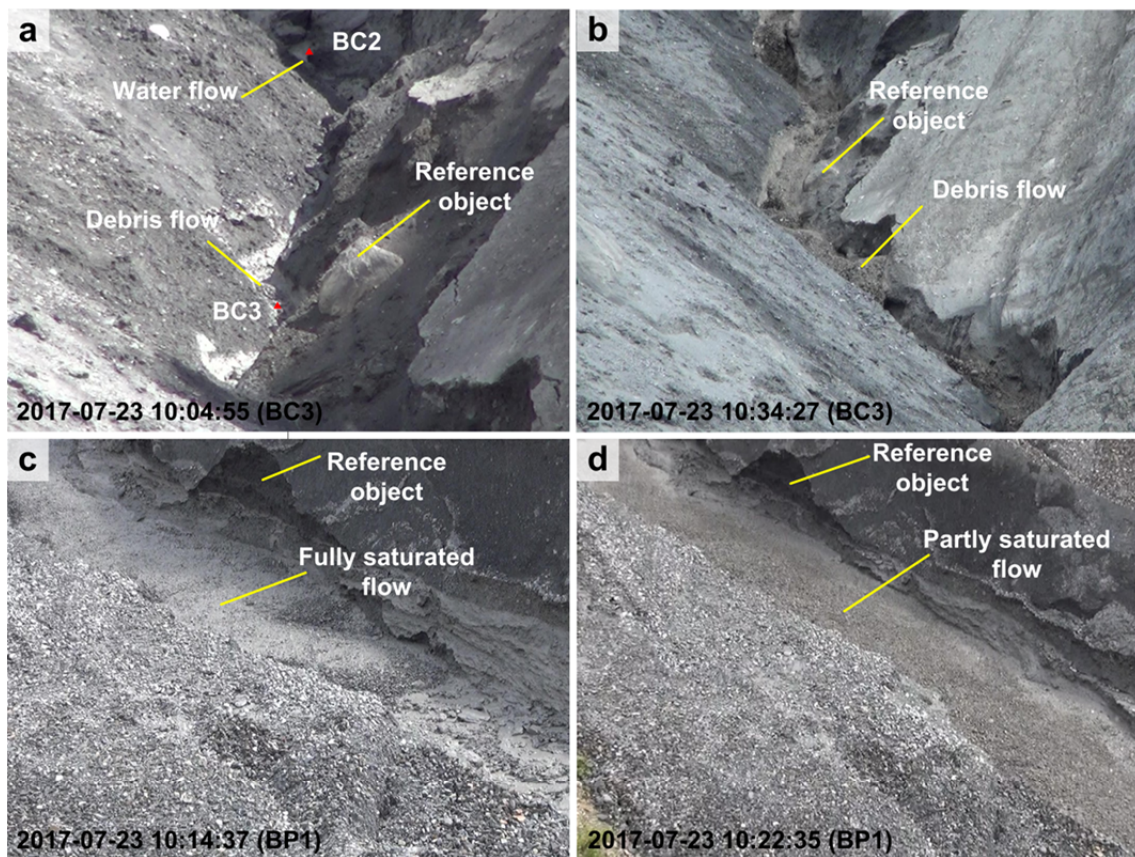


**Fig. 10** Video images showing debris surges with different volume (a, b) and different water content (c, d) on July 23, 2017 in sub-watershed B. Location of the framed area is listed in the bracket.

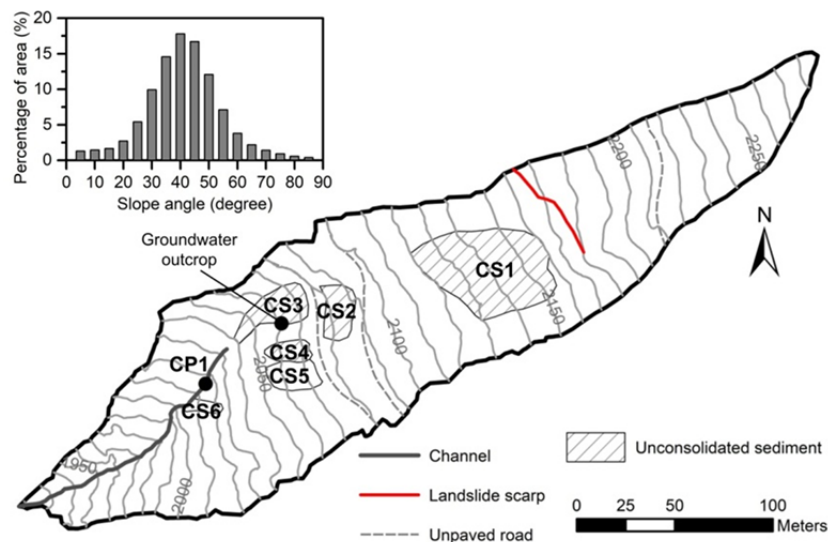


**Fig. 11** Terrain of sub-watershed C.

occurred on the slope located on the right bank of the channel. The mobilized debris travelled downstream along the slope and fell on the surface of the passing debris flow in the channel. At 14:03, a surge of debris flow was recorded in the rill connecting slope CS3 and

the channel. At 15:24, a failure occurred on slope CS5. Most of the mobilized sediment temporarily deposited on the downstream slope (CS6), and was further eroded by channel runoff, generating some surges of debris flow. Meanwhile, this rainfall event triggered

some small landslides in areas CS1 and CS2, a part of which converted to debris flows (Fig. 13d).

## 5 Discussions

### 5.1 Debris-flow initiation mechanism in the Jiangjia Gully

Landslides, mainly controlled by the infiltration process, play important roles in sediment supply for debris-flow occurrence in the study area. When landslides are triggered, a part of landslide sediment immediately enters the channel and is then mobilized by channel erosion, as observed in sub-watershed B. The remaining part accumulates on hillslopes and takes part in debris-flow activities in subsequent rainfall events in three manners: (1) directly transforming into debris flows after further failure; (2) rill erosion; and (3) releasing sediment to channels after further failure, as observed in sub-watersheds A and C. In these processes, concentrated water flow is

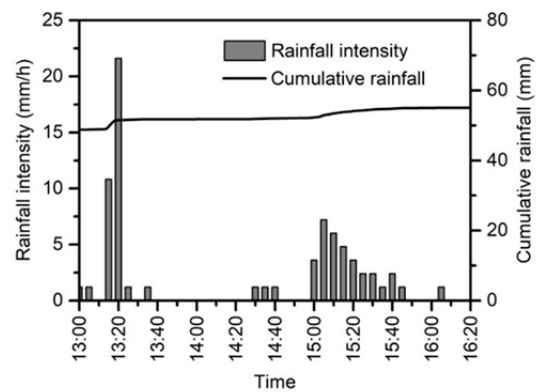


**Fig. 12** Rainfall intensity at 5-minute intervals and cumulative rainfall recorded by R4 during 13:00-16:20 on August 25, 2017.

usually necessary for sediment transport. Consequently, both infiltration-dominated processes and runoff-dominated processes are important in debris-flow initiation. Nonetheless, the *I-D* threshold in Menqian Gully is comparable to those derived from some instrumented runoff-dominated basins prone to debris flows in Europe and in the USA (Fig. 14).

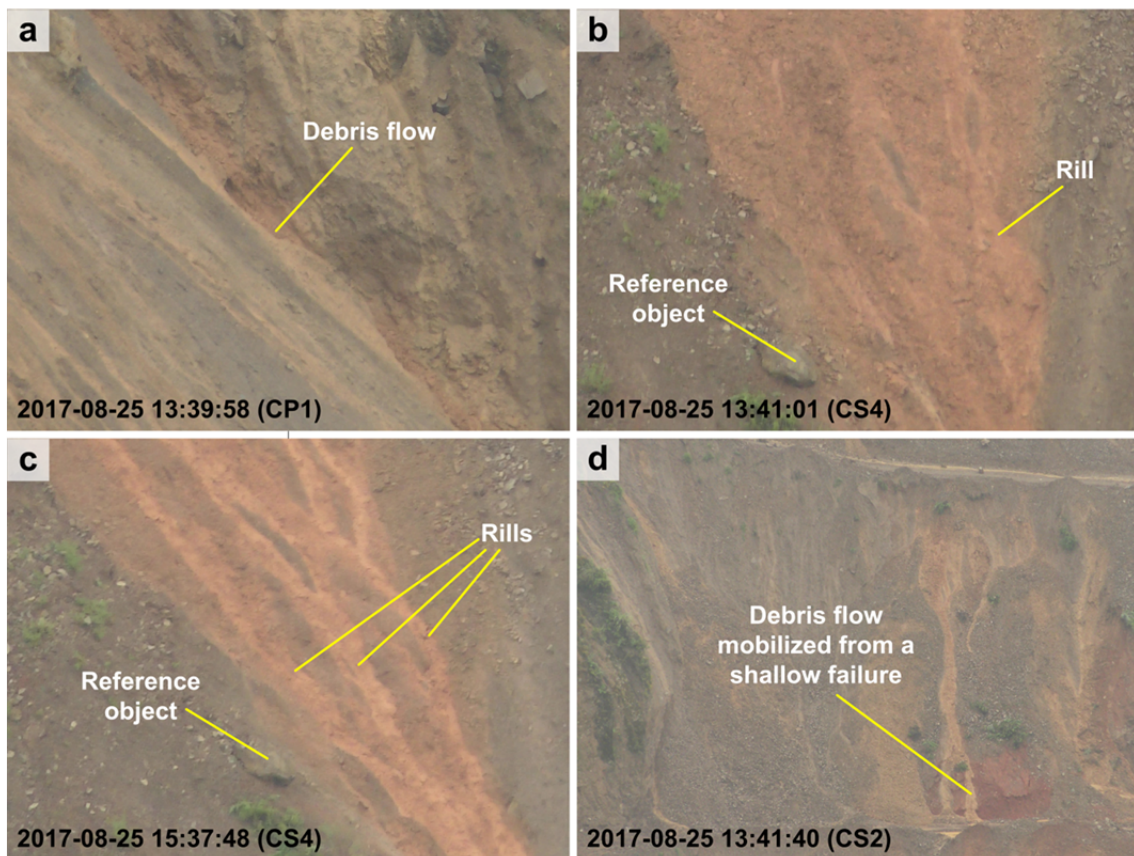


**Fig. 13** Video images showing a surge of debris flow in the channel (a), rills on slope CS4 observed at 13:41 (b) and at 15:37 (c), and a surge of debris flow mobilized from a shallow failure (d) on August 25, 2017 in sub-watershed C. Location of the framed area is listed in the bracket.



Once landslides provide abundant sediment to a channel, the channel becomes transport limited, which means that debris flows will be triggered if the flow discharge surpasses a threshold. Due to steep channel gradients ( $> 20^\circ$ ) in most sub-watersheds, the threshold is relatively small, as observed in sub-watershed B. Another case was found in a 0.19-km<sup>2</sup> sub-basin near sub-watershed A, where a debris surge was observed at 13:45 on August 26, 2017, 9.5 hours after the rain stopped, because the steep channel ( $23.8^\circ$ ) was filled with landslide accumulations generated in the August 25 rainfall event (Appendix 2). Antecedent rainfall plays nonnegligible roles in triggering landslides as it reduces soil suction (Caracciolo et al. 2017). Therefore, more antecedent rainfall usually means more sediment supply in the channel and thus lower 10-minute triggering rainfall in the study area (Fig. 5B). In contrast, antecedent rainfall is negligible and debris flows are merely related with high-intensity rainfall bursts in some runoff-dominated torrents (Deganutti et al. 2000; Coe et al. 2008).

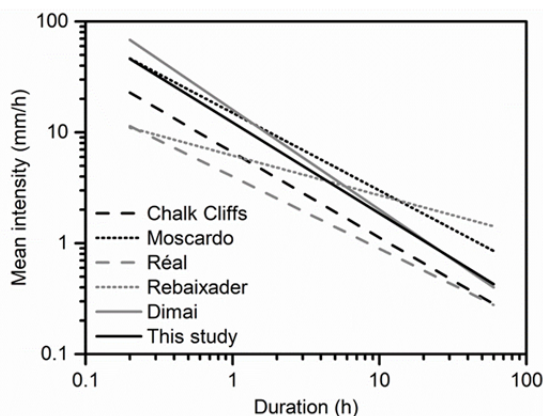


**Fig. 14** Comparison of  $I$ - $D$  threshold in Menqian Gully with other sites including Chalk Cliffs in the USA (Coe et al. 2008), the Moscardo Torrent in Italy (Deganutti et al. 2000), the Dimai Basin in Italy (Berti et al. 2020), the Réal Torrent in France (Bel et al. 2017), and the Rebaixader catchment in Spain (Abancó et al. 2016).

It is most likely that sediment is not only provided by landslides, rill erosion, and gully erosion in debris-flow triggering rainfall events, but also supplied by these processes in non-triggering rainfall events, and by rockfall and dry ravel in the dry period. As a result, a long-term sediment accumulation facilitates debris-flow occurrence. For instance, the first debris-flow event was triggered on August 10 in 2016, when masses of sediment had accumulated in

the channel in the preceding dry season (winter and spring) and early summer. In contrast, no debris flows were recorded in the rainfall event on August 15, 2016 for the absence of enough preexisting sediment supply, although both the  $I$ - $D$  threshold and the  $R_{10min}$ - $AR$  threshold were exceeded ( $I=1.46$  mm/h,  $D=21.17$  h,  $R_{10min}=6.1$  mm, and  $AR=36.4$  mm).

## 5.2 Factors facilitating movement of partly saturated flow in the Jiangjia Gully

Partly saturated flow was frequently observed in the sub-watersheds of the Jiangjia Gully. Maintenance of the flow is mainly attributed to high channel gradients. For a uniform layer of saturated bed sediment where surface water flow is absent, the shear stress is written as (Takahashi 1978; Imaizumi et al. 2017):

$$\tau = [\rho_w + (\rho_s - \rho_w)C_v]gh\cos\theta\sin\theta \quad (2)$$

where  $\rho_w$  and  $\rho_s$  represent the bulk density of water and solid particles;  $C_v$  is solid volumetric concentration;  $g$  is gravitational acceleration;  $h$  is sediment depth; and  $\theta$  is slope angle of the channel. Assuming that cohesion strength and lateral resistance are negligible, the resisting stress is written as:

$$\tau_r = (\rho_s - \rho_w)C_vgh\cos^2\theta\tan\varphi \quad (3)$$

where  $\varphi$  is internal friction angle. Given that  $\rho_s = 2650$  kg/m<sup>3</sup>,  $C_v = 0.64$  (corresponding to a dry bulk density of 1700 kg/m<sup>3</sup>), and  $\varphi$  is equal to the natural angle of repose in the study area ( $\sim 38^\circ$ ), we can deduce that  $\tau$  is larger than  $\tau_r$  if  $\theta$  is greater than  $21.9^\circ$ . It means that saturation is not required for the mobilization of sediment in channels steeper than a threshold. This is consistent with findings of Imaizumi et al. (2017) in a debris-flow initiation zone in Japan, where partly saturated flows tend to form steeper channel sections ( $22.2^\circ$ - $37.3^\circ$ ) while fully saturated debris flows tend to form gentler channel sections ( $< 22.2^\circ$ ). Prancevic et al. (2014) also found that debris flow is initiated from channel bed failure rather than fluvial transport when the channel slope is beyond  $\sim 22^\circ$  in their laboratory experiments.

Nonetheless, a surface water flow is usually required for the formation of a debris-flow surge in steep channels. It provides water to the bed sediment before the failure of the sediment while transforming into a muddy flow and exerting pressure behind the partly saturated front after the sediment is mobilized.

This phenomenon was observed in sub-watersheds A and B. It was also reported in the Cancia basin in eastern Italian Alps, where the slope angle is about 30° in the initiation zone of debris flow (Simoni et al. 2020).

In addition, debris-flow runout distance can be enhanced by coalescence of multiple surges. When a debris surge deposits in the channel and induces temporary damming, it will increase in volume with the arrival of subsequent surges, and then is restarted by gravity and impact pressure, as observed in sub-watershed A. Existing research has revealed that travel distances of landslides and debris flows increase with debris volume (Staron and Lajeunesse 2009; de Haas et al. 2015; Hürlimann et al. 2015). Therefore, the enlarged renewed surge is expected to exhibit higher runout distance.

Moreover, the formation of levee is favorable to the movement of debris flow. Lateral levees were formed in the channel when partly saturated flow travelled forward (Fig. 8A), which means that high-friction, coarse-grained snouts were displaced laterally by subsequent finer material that had lower friction (Johnson et al. 2012).

Furthermore, excess pore fluid pressure is expected to play an important role in the propagation of partly saturated flow. Excess pore fluid pressure has been observed at the bottom of debris flow in large-scale experiments and in natural torrents (Iverson 2003; McCoy et al. 2010). Although there were no observation data on fluid pressure in the present study, the low bearing capacity of the fresh partly saturated deposit demonstrates the presence of excess pore fluid pressure (Appendix 3).

## 6 Conclusions

To study debris-flow formation mechanism in the Jiangjia Gully, field observations of debris-flow activities in the initiation zone were performed and the related rainfall data were analyzed. It shows that landslides constituted an important source for sediment supply. Some landslides, usually triggered on talus slopes, directly evolved into debris flows, while sediment mobilized by the other landslides entered rills and channels, and was finally entrained by concentrated water flow. Therefore, both infiltration-dominated processes and runoff-dominated processes are important in debris-flow

initiation in the study area.

In contrast to some active runoff-dominated basins, where rainfall conditions for debris-flow triggering are represented by intensity-duration thresholds while antecedent rainfall is negligible, rainfall threshold in the study area can be described both by a power-law relationship between mean intensity and duration and by a linear relationship between peak 10-minute rainfall and antecedent rainfall. False alarms will be greatly reduced if these two thresholds are used together. Moreover, rainfall data recorded by different gauges usually exhibit great variance. The debris-flow event is expected to be larger in volume when records from all gauges exceed the threshold.

Since sediment was supplied discontinuously, debris flows were typically initiated in surges. In a specific sub-watershed, debris flows might vary in moisture content and volume from surge to surge during a rainfall event. Partly saturated flows were frequent in the sub-watersheds for high channel gradients (>20°). Their mobility was facilitated by coalescence of multiple surges, formation of lateral levees, and existence of excess pore fluid pressure. Initiation of debris flow is a complex process in the Jiangjia Gully. To quantitatively reveal the process, instruments need to be installed in typical sub-watersheds in future to measure rainfall, soil moisture, flow depth and velocity to capture the whole process from mass movement on hillslopes to sediment transport in channels.

## Acknowledgements

The authors sincerely appreciate the valuable comments from the anonymous reviewers. We are grateful to LI Xiaoyu, WEI Li, YANG Taiqiang, XIA Manyu, YANG Chaoping from Institute of Mountain Hazards and Environment, Chinese Academy of Sciences, and SHI Cetu, XU Tianbao, XU Cong from Chengdu University of Information Technology for their cooperation in field observation and survey. The Dongchuan Debris Flow Observation and Research Station, Chinese Academy of Sciences is acknowledged for rainfall and topographic data supply. This work is financially supported by the National Key Research and Development Program of China (2020YFD1100701), the Science and Technology Research and Development Program of

China Railway (K2019G006), and the Chongqing Municipal Bureau of Land, Resources and Housing Administration (KJ-2021016).

**Electronic supplementary material:**

Supplementary material ([Appendixes 1–3](#)) is available in the online version of this article at <https://doi.org/10.1007/s11629-021-7292-3>

## References

- Abancó C, Hürlimann M, Moya J, et al. (2016) Critical rainfall conditions for the initiation of torrential flows. Results from the Rebaixader catchment (Central Pyrenees). *J Hydrol* 541: 218–229. <https://doi.org/10.1016/j.jhydrol.2016.01.019>
- Badoux A, Graf C, Rhyner J, et al. (2009) A debris-flow alarm system for the Alpine Illgraben catchment: design and performance. *Nat Hazards* 49: 517–539. <https://doi.org/10.1007/s11069-008-9303-x>
- Bel C, Liébault F, Navratil O, et al. (2017) Rainfall control of debris-flow triggering in the Réal Torrent, Southern French Prealps. *Geomorphology* 291: 17–32. <https://doi.org/10.1016/j.geomorph.2016.04.004>
- Berger C, McArdell BW, Fchlunegger F (2011) Direct measurement of channel erosion by debris flows, Illgraben, Switzerland. *J Geophys Res* 116: F01002. <https://doi.org/10.1029/2010JF001722>
- Berti M, Genevois R, Simoni A, et al. (1999) Field observations of a debris flow event in the Dolomites. *Geomorphology* 29: 265–274. [https://doi.org/10.1016/S0169-555X\(99\)00018-5](https://doi.org/10.1016/S0169-555X(99)00018-5)
- Berti M, Bernard M, Gregoretti C, et al. (2020) Physical interpretation of rainfall thresholds for runoff-generated debris flows. *J Geophys Res-Earth* 125: e2019JF005513. <https://doi.org/10.1029/2019JF005513>
- Bezák N, Šraj M, Mikoš M (2016) Copula-based IDF curves and empirical rainfall thresholds for flash floods and rainfall-induced landslides. *J Hydrol* 541: 272–284. <https://doi.org/10.1016/j.jhydrol.2016.02.058>
- Caracciolo D, Arnone E, Conti FL, et al. (2017) Exploiting historical rainfall and landslide data in a spatial database for the derivation of critical rainfall thresholds. *Environ Earth Sci* 76: 1–16. <https://doi.org/10.1007/s12665-017-6545-5>
- Chen NS, Zhou W, Yang CL, et al. (2010) The processes and mechanism of failure and debris flow initiation for gravel soil with different clay content. *Geomorphology* 121: 222–230. <https://doi.org/10.1016/j.geomorph.2010.04.017>
- Chen X, Cui P, Feng Z, et al. (2006) Artificial rainfall experimental study on landslide translation to debris flow. *Chin J Rock Mech Eng* 25: 106–116. (In Chinese) <https://doi.org/10.3321/j.issn:1000-6915.2006.01.018>
- Coe JA, Kinner DA, Godt JW (2008) Initiation conditions for debris flows generated by runoff at Chalk Cliffs, central Colorado. *Geomorphology* 96: 270–297. <https://doi.org/10.1016/j.geomorph.2007.03.017>
- Comiti F, Marchi L, Macconi P, et al. (2014) A new monitoring station for debris flows in the European Alps: first observations in the Gadria basin. *Nat Hazards* 73: 1175–1198. <https://doi.org/10.1007/s11069-014-1088-5>
- Cui P, Chen X, Wang Y, et al. (2005) Jiangjia Ravine debris flows in the south-western China. In: Jakob M, Hungr O (eds.), *Debris-flow Hazards and Related Phenomena*. Springer, Berlin. pp 565–594. [https://doi.org/10.1007/3-540-27129-5\\_22](https://doi.org/10.1007/3-540-27129-5_22)
- Cui P, Guo X, Yan Y, et al. (2018) Real-time observation of an active debris flow watershed in the Wenchuan Earthquake area. *Geomorphology* 321: 153–166. <https://doi.org/10.1016/j.geomorph.2018.08.024>
- De Haas T, Braat L, Leuven JRFW, et al. (2015) Effects of debris flow composition on runout, depositional mechanisms, and deposit morphology in laboratory experiments. *J Geophys Res-Earth* 120: 1949–1972. <https://doi.org/10.1002/2015JF003525>
- Deganutti AM, Marchi L, Arattano M (2000) Rainfall and debris flow occurrence in the Moscardo basin (Italian Alps). In: Wiecek GF, Naeser ND (eds.), *Debris-Flow Hazards Mitigation: Mechanics, Prediction, and Assessment*. Balkema, Rotterdam. pp 67–72.
- Gianecchini R, Galanti Y, D'Amato Avanzi G, et al. (2016) Probabilistic rainfall thresholds for triggering debris flows in a human-modified landscape. *Geomorphology* 257: 94–107. <https://doi.org/10.1016/j.geomorph.2015.12.012>
- Gregoretti C (2008) Inception sediment transport relationships at high slopes. *J Hydraul Eng-ASCE* 134(11): 1620–1629. [https://doi.org/10.1061/\(ASCE\)0733-9429\(2008\)134:11\(1620\)](https://doi.org/10.1061/(ASCE)0733-9429(2008)134:11(1620))
- Gregoretti C, Dalla Fontana G (2008) The triggering of debris flow due to channel-bed failure in some alpine headwater basins of the Dolomites: analyses of critical runoff. *Hydrol Process* 22: 2248–2263. <https://doi.org/10.1002/hyp.6821>
- Guo X, Li Y, Cui P, et al. (2020) Intermittent viscous debris flow formation in Jiangjia Gully from the perspectives of hydrological processes and material supply. *J Hydrol* 589: 125184. <https://doi.org/10.1016/j.jhydrol.2020.125184>
- Guzzetti F, Peruccacci S, Rossi M, et al. (2008) The rainfall intensity–duration control of shallow landslides and debris flows: an update. *Landslides* 5: 3–17. <https://doi.org/10.1007/s10346-007-0112-1>
- Hürlimann M, McArdell BW, Rickli C (2015) Field and laboratory analysis of the runout characteristics of hillslope debris flows in Switzerland. *Geomorphology* 232: 20–32. <https://doi.org/10.1016/j.geomorph.2014.11.030>
- Imaizumi F, Hayakawa YS, Hotta N, et al. (2017) Relationship between the accumulation of sediment storage and debris-flow characteristics in a debris-flow initiation zone, Ohya landslide body, Japan. *Nat Hazard Earth Sys* 17: 1923–1938. <https://doi.org/10.5194/nhess-17-1923-2017>
- Imaizumi F, Masui T, Yokota Y, et al. (2019) Initiation and runout characteristics of debris flow surges in Ohya landslide scar, Japan. *Geomorphology* 339: 58–69. <https://doi.org/10.1016/j.geomorph.2019.04.026>
- Iverson RM (2003) The debris-flow rheology myth. In: Rickenmann D, Chen, CL (eds.), *Debris-Flow Hazards Mitigation: Mechanics, Prediction, and Assessment*. Millpress, Rotterdam. pp 303–314.
- Iverson RM, Reid ME, LaHusen RG (1997) Debris-flow mobilization from landslides. *Annu Rev Earth Pl Sc* 25: 85–138. <https://doi.org/10.1146/annurev.earth.25.1.85>
- Jiang X, Cui P, Chen H, et al. (2017) Formation conditions of outburst debris flow triggered by overtopped natural dam failure. *Landslides* 14: 821–831. <https://doi.org/10.1007/s10346-016-0751-1>
- Jiang Z, Fan X, Subramanian SS, et al. (2021) Probabilistic rainfall thresholds for debris flows occurred after the Wenchuan earthquake using a Bayesian technique. *Eng Geol* 280: 105965. <https://doi.org/10.1016/j.enggeo.2020.105965>
- Johnson CG, Kokelaar BP, Iverson RM, et al. (2012) Grain-size segregation and levee formation in geophysical mass flows. *J of Geophys Res* 117: F01032.

- <https://doi.org/10.1029/2011JF002185>
- Johnson KA, Sitar N (1990) Hydrologic conditions leading to debris-flow initiation. *Can Geotech J* 27: 789-801.  
<https://doi.org/10.1139/t90-092>
- Kean JW, Staley DM, Cannon SH (2011) In situ measurements of post-fire debris flows in southern California: comparisons of the timing and magnitude of 24 debris-flow events with rainfall and soil moisture conditions. *J Geophys Res* 116: F04019. <https://doi.org/10.1029/2011JF002005>
- Kean JW, McCoy SW, Tucker GE, et al. (2013) Runoff-generated debris flows: observations and modeling of surge initiation, magnitude, and frequency. *J Geophys Res* 118: 2190-2207.  
<https://doi.org/10.1002/jgrf.20148>
- Liu J, Zhang L, Du Y (2020) Seismic hazard assessment of the mid - northern segment of Xiaojiang fault zone in southwestern China using scenario earthquakes. *B Seismol Soc Am* 110: 1191-1210.  
<https://doi.org/10.1785/0120190248>
- McCoy SW, Kean JW, Coe JA, et al. (2010) Evolution of a natural debris flow: In situ measurements of flow dynamics, video imagery, and terrestrial laser scanning. *Geology* 38: 735-738. <https://doi.org/10.1130/G30928.1>
- McCoy SW, Kean JW, Coe JA, et al. (2012) Sediment entrainment by debris flows: In situ measurements from the headwaters of a steep catchment. *J of Geophys Res* 117: F03016. <https://doi.org/10.1029/2011JF002278>
- Prancevic JP, Lamb MP, Fuller BM (2014) Incipient sediment motion across the river to debris-flow transition. *Geology* 41: 191-194.  
<https://doi.org/10.1130/G34927.1>
- Reid ME, LaHusen RG, Iverson RM (1997) Debris-flow initiation experiments using diverse hydrologic triggers. In: Chen C-L (ed), *Debris-Flow Hazards Mitigation: Mechanics, Prediction, and Assessment*. ASCE, New York. pp 1-11.
- Rickenmann D (1999) Empirical relationships for debris flows. *Nat Hazards* 19: 47-77.  
<https://doi.org/10.1023/A:1008064220727>
- Schuster RL (2000) Outburst debris-flows from failure of natural dams. In: Wieczorek GF, Naeser ND (eds.), *Debris-Flow Hazards Mitigation: Mechanics, Prediction, and Assessment*. Balkema, Rotterdam. pp 29-42.
- Shi Z, Wang G (2017) Evaluation of the permeability properties of the Xiaojiang Fault Zone using hot springs and water wells. *Geophys J Int* 209: 1526-1533.  
<https://doi.org/10.1093/gji/ggx113>
- Simoni A, Bernard M, Berti M, et al. (2020) Runoff - generated debris flows: observation of initiation conditions and erosion - deposition dynamics along the channel at Cancia (eastern Italian Alps). *Earth Surf Process Landf* 45: 3556-3571.  
<https://doi.org/10.1002/esp.4981>
- Staron L, Lajeunesse E (2009) Understanding how volume affects the mobility of dry debris flows. *Geophys Res Lett* 36: L12402.  
<https://doi.org/10.1029/2009GL038229>
- Suwa H, Okunishi K, Sakai M (1993) Motion, debris size and scale of debris flows in a valley on Mount Yakedake, Japan. In: Hadley RF, Mizuyama T (eds.), *Sediment Problems: Strategies for Monitoring, Prediction and Control*. IAHS, Wallingford. pp 239-248.
- Takahashi T (1978) Mechanical characteristics of debris flow. *J Hydr Div* 104: 1153-1169.  
<https://doi.org/10.1061/JYCEAJ.0005046>
- Takahashi T (2007) *Debris Flow: Mechanics, Prediction and Countermeasures*. Taylor and Francis, Balkema, Leiden.
- Tang C, Rengers N, van Asch TWJ, et al. (2011) Triggering conditions and depositional characteristics of a disastrous debris flow event in Zhouqu city, Gansu Province, northwestern China. *Nat Hazard Earth Sys* 11: 2903-2912.  
<https://doi.org/10.5194/nhess-11-2903-2011>
- Tognacca C, Bezzola GR, Minor HE (2000) Threshold criterion for debris flow initiation due to channel-bed failure. In: Wieczorek GF, Naeser ND (eds.), *Debris-Flow Hazards Mitigation: Mechanics, Prediction, and Assessment*. Balkema, Rotterdam. pp 89-97.
- Wang B, Li Y, Liu D, et al. (2018) Debris flow density determined by grain composition. *Landslides* 15: 1205-1213.  
<https://doi.org/10.1007/s10346-017-0912-x>
- Wang F, Sassa K (2007) Initiation and traveling mechanisms of the May 2004 landslide-debris flow at Bettou-dani of the Jinnosuke-dani landslide, Haku-san Mountain, Japan. *Soils Found* 47: 141-152.  
<https://doi.org/10.3208/sandf.47.141>
- Wang Y, Cui P, Wang Z, et al. (2017) Threshold criterion for debris flow initiation in seasonal gullies. *Int J Sediment Res* 32: 231-239.  
<https://doi.org/10.1016/j.ijsrc.2017.03.003>
- Zhang S (1993) A comprehensive approach to the observation and prevention of debris flows in China. *Nat Hazards* 7: 1-23.  
<https://doi.org/10.1007/BF00595676>
- Zhuang J, Cui P, Wang G, et al. (2015) Rainfall thresholds for the occurrence of debris flows in the Jiangjia Gully, Yunnan Province, China. *Eng Geol* 195: 335-346.  
<https://doi.org/10.1016/j.enggeo.2015.06.006>